ORIGINAL ARTICLE

Dosimetric evaluation of PLA and ABS materials produced by two different production techniques

Songül Çavdar Karaçam[1] · Duygu Tunçman[1] · Tülin Şahin[2] · Şenol Şahin[2] · Şefika Arzu Ergen[3] ·
Meltem Dağdelen[3] · Ömer Erol Uzel[3] · Didem Çolpan Öksüz[3] · Ghada Almisned[4] · H. O. Tekin[5,6]

Abstract

In radiotherapy applications, with the aim of accurately delivering the prescribed dose in-patient treatments, a wide variety of organic and/or inorganic materials can be utilized as bolus material. In recent years, polymer materials have become a wide range of scientific research in radiotherapy. Especially, PLA (polylactic acid) and acrylonitrile butadiene styrene (ABS) materials are widely utilized in various applications within the field of radiotherapy. While three-dimensional (3D) printing, especially using fused deposition modeling (FDM) technology, was among the first techniques adopted, plastic injection molding (IM) has also been a well-established manufacturing method for many years. Initially, ABS and PLA materials were 3D-printed on an FDM 3D printer as square prisms measuring $12 \times 12 \times 1$ cm^3. These were specifically designed for use as measurement instruments in radiation assessments. Subsequently, identical test materials were produced through IM in an ISO D2–type mold made of S235JR steel (material number 1.0038) with the same dimensions. In radiotherapy applications, it is important for clinical use to evaluate the material of dosimetric properties as well as tissue equivalence. The goal was to dosimetrically evaluate the response of these materials to radiation produced by both FDM and IM techniques. Hounsfield units (HU) values were determined with the CT simulator device for all materials. Dosimetric measurements were performed using a 6-MV nominal photon energy. Percentage depth doses, dose profiles, and radio transmittance measurements of the materials were conducted in a water phantom and solid water phantom. All measurements were also conducted for commercially available bolus materials used in patients. Commercial bolus was used as a reference due to its routine use in the clinic. Although the dosimetric parameters for materials produced through 3D printing and plastic injection molding yielded similar results among themselves and with bolus material, it is advisable to evaluate the material dosimetrically before its use as a personal material on a patient due to printing characteristics and material variability.

Keywords 3D printer · Radiotherapy · Dosimetry · Plastic injection molding

1 Introduction

Bolus materials are tissue-equivalent materials used to correct irregular patient contours in clinical radiation therapy. One of the most critical parameters in the selection of bolus material is the surface anatomy of the tissue. The dose delivered to a flat surface versus the curvatures on the patient's surface alters the dose distribution [1, 2]. The chosen bolus material should conform to the skin surface, be non-toxic, not degrade under radiation in photon and electron therapy, not be adhesive, and its surface quality should not deteriorate during treatment. For this purpose, materials from the thermoplastic, elastomer, and/or thermoplastic elastomer

groups are used as bolus material [3]. In addition to commercially available bolus in radiotherapy, different production techniques are available in recent years depending on the chosen material type. Depending on the type of bolus material, hand production in a mold, molding on the tissue surface of the patient, injection molding, casting, and additive manufacturing (3D) are the most commonly used production methods [4, 5].

3D printing is a rapidly advancing technology with significant potential to influence various medical applications, including patient-specific implants or prostheses, surgical guides, and its use as a research and educational training tool. Moreover, in radiotherapy, 3D printing technology is notable. The studies published in the recent years have investigated the utilization of 3D printing technologies for

---

Extended author information available on the last page of the article

جامعة قطر
QATAR UNIVERSITY

🌐 Springer

the manufacturing of varied patient-specific equipment in the field of radiotherapy, Rooney et al. declare that the most frequently reported 3D printing applications comprise phantoms for quality assurance (26%), production of bolus material (17%), applicators for brachytherapy (20%), compensators (7%), animal irradiations for preclinical research (10%), and design for immobilization devices (5%) [6–10].

The inherent characteristics of high-energy photon beams, which tend to spare the skin, can lead to insufficient radiation dosage for superficial lesions. To address this issue, a layer of material, commonly referred to as a "bolus," is frequently used on the skin's surface. This technique enhances the radiation dose reaching the skin, thereby improving the effectiveness of treating superficial lesions [11]. However, the surface roughness of the material, which leads to the formation of air gaps between the patient's skin, hinders the use of commercially available boluses. Additionally, the fixed thickness in the geometry of commercial boluses poses challenges for certain issues. In contrast to commercially available flat boluses, 3D-printed boluses offer a more precise conformity to the patient's skin surface [12, 13]. The effectiveness of patient-specific 3D-printed boluses in radiotherapy stems from their ability to closely adhere to the skin.

3D printing technology has become the leading rapid prototyping technology for creating well-defined and complex 3D structures. The prevalent additive manufacturing method, commonly referred to as 3D printing, is a popular approach in the specialized manufacturing sector, employing fused deposition modeling (FDM). FDM is extensively utilized due to its user-friendly nature, rapid processing, simplicity, and cost-effectiveness. It represents a straightforward additive manufacturing technique where thermoplastic filaments are extruded through a circular die to sequentially construct 3D objects layer by layer. This enables the creation of intricate structures with the necessary dimensional and geometric precision.

The materials used are provided in the form of filaments [14]. A variety of polymers, such as polylactic acid (PLA), acrylonitrile butadiene styrene (ABS), polyamide, polycarbonate (PC), high-density polyethylene (HDPE), and thermoplastic polyether urethane (TPU), is produced through the fused deposition modeling (FDM) process. In recent years, polymer materials have garnered considerable attention in scientific research related to radiotherapy. Particularly, PLA and ABS materials find widespread use in various radiotherapy applications. However, there is a possibility of void formation in polymer products created via this technique, attributed to inadequate diffusion at the interfaces during the manufacturing process. Extensive research has been conducted to modify processing parameters, such as temperature, air gaps, layer thickness, and infill density, aiming to improve the quality of the final product [8, 14]. The broad spectrum of materials used in 3D printing and the numerous variables involved in the preparation process pose challenges for its application in radiotherapy, as these factors can affect the dosage. Consequently, it is essential to develop more thorough evaluation methods, including real-patient validations and dosimetric analyses, to effectively incorporate 3D printing technology in clinical practice. Although extensive research has been carried out to refine the processing parameters of fused deposition modeling (FDM) to enhance product performance, a notable concern remains regarding the expected reduction in physical and mechanical properties when compared to products made via injection molding. In light of this, the authors suggest a comparative study of the dosimetric properties of commonly utilized materials like polylactic acid (PLA) and acrylonitrile butadiene styrene (ABS), processed through both FDM and injection molding (IM). This comparison aims to elucidate the differences in dosimetric properties that arise from the distinct processing methods employed in FDM. Such an analysis is vital for realizing the full capabilities of FDM-produced products, especially in considering their potential to substitute for items traditionally manufactured through injection molding. Several articles have reported on the comparative investigation of parts modeled by FDM and injection molding [14–17]. However, the majority of the literature primarily focuses on the physical and mechanical properties of polymers. Notably, there is a lack of comparative dosimetric analysis for parts manufactured using FDM and IM specifically for radiotherapy applications. To address this gap, our study includes dosimetric comparisons between these materials, which can be utilized as boluses, and commercially available bolus products.

In this research, FDM printing parameters were employed to produce samples of PLA and ABS. Additionally, injection-molded samples were prepared for comparative analysis. Measurements of Hounsfield units (HU), percentage depth dose (PDD), and dose profile for the samples were conducted and compared between the FDM and injection molding methods.

2 Material and method

2.1 Printing of samples

In this investigation, $12 \times 12 \times 1$ cm^3 (L×W×H) cubic samples were 3D-printed using PLA and ABS filaments. The cubic models were sliced using Cura, which is a 3D printing slicer software specifically designed for FDM printing (Fig. 1a).

The samples were produced using the Ultimaker S5 3D printer, with the printing parameters configured to a nozzle temperature of 200 °C and a flow rate set at 100%. Filaments from the same manufacturer, specifically Ultimaker PLA and

Fig. 1 FDM machine (**a**) and IM machine (**b**) used in production
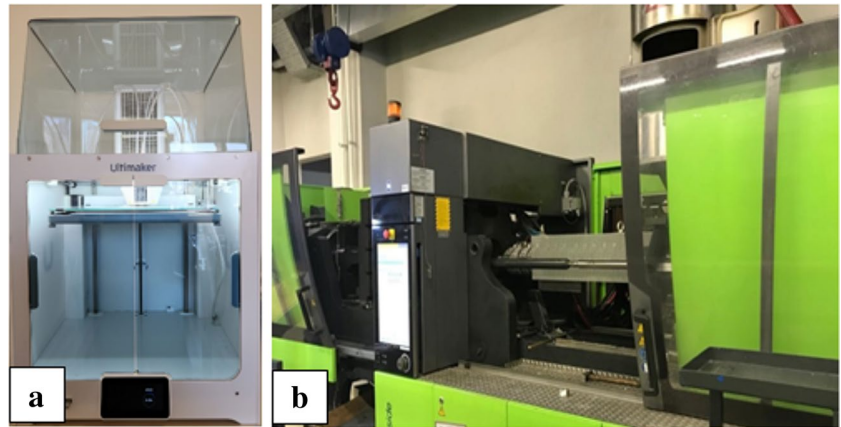
Ultimaker ABS, were employed to ensure consistency. For both materials, the infill density was uniformly set at 100%. Furthermore, the "lines" pattern was selected for the infill, with an infill layer thickness of 0.3 mm for both materials. This infill pattern was chosen primarily for its superior surface quality, which is crucial when applied to the patient's skin, reflecting the importance of high surface quality in the print settings, as indicated by the literature [18]. For comparison purposes, plastic injection molded samples were also prepared.

For an alternative to commercially produced bolus via casting, ABS and PLA materials were selected for two different methods. These materials possess similar chemical structures and mechanical properties but exhibit differing rheological characteristics due to the requirements of the production technology. The ABS, characterized by its natural color and particulate structure, was acquired from Sabic under the brand name CYCOLAC RESIN. As the secondary material for evaluation, the PLA was procured in its particulate form from INGEO, branded as Biopolymer 3052D. The production for both materials was made on the Engel Victory 330/50 Tech plastic injection molding machine shown in Fig. 1b. In addition, a high-precision process chiller (Frigel

Microgel Duo) with a temperature control unit was used to keep the mold temperature constant at the specified (set) temperature for each test piece in each sample. Samples were produced by direct injection molding in an ISO D2 type mold made of S235JR steel (material number 1.0038) according to ISO 294–3. A total of four materials were produced and used for the study.

Dosimetric measurements were performed using commercial bolus material for reference. Commercial bolus density is 1.03 g/cm³ (CIVCO Medical Solution, Orange City, FL, USA), and its main component is polymer gel. The commercial bolus dimensions is $40 \times 40 \times 1$ cm³.

2.2 Hounsfield unit (HU) analysis

General electric discovery RT (GE Healthcare, Milwaukee, USA) computed tomography (CT) simulator was utilized for assessing the Hounsfield unit (HU) value of the materials (Fig. 2.).

Within the CT simulator device, the attenuation value (μ_x) of each voxel is transformed into a numerical value known as the relative Hounsfield unit, determined on the

Fig. 2 Samples and CT device. **a** Top left PLA and top right ABS (FDM); bottom left is a sample of PLA and bottom right is ABS (IM). **b** Commercial bolus
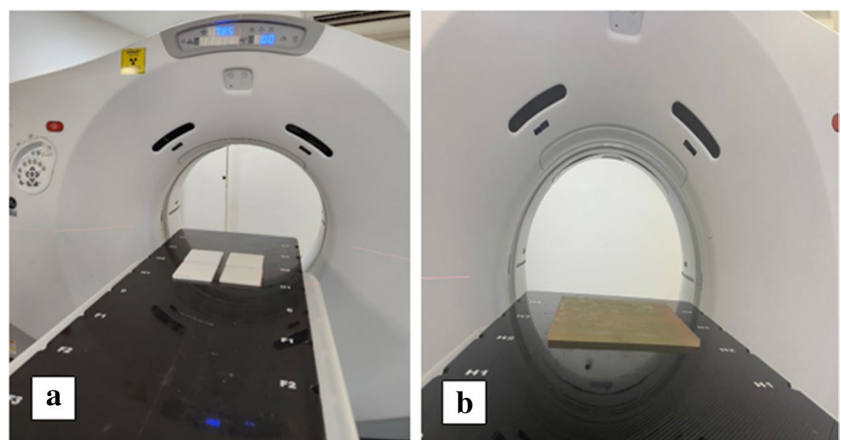
basis of the attenuation coefficient (μ_w) of water as calculated by the formula provided below (Eq. 1).

$$HU = 1000 \cdot [(\mu_x - \mu_w/\mu_w)] \tag{1}$$

Various shades of gray are employed to depict numerical data. In the visualization, the HU value of air is depicted as black, positioned at the leftmost end of the scale, whereas the value at the rightmost end of the scale is typically depicted as white, symbolizing dense materials like calcium and metal. The middle gray value on this scale represents water, defined by an HU value of 0 [19].

Every pixel in a computed tomography (CT) image is linked to a Hounsfield unit (HU) value, which acts as a measure of the radiation absorption coefficient of the object being imaged. In the CT image (Fig. 3), the average HU values and their standard deviation (STD) were collected from five distinct positions ($+10$ cm, $+5$ cm, center, -5 cm, -10 cm). This was done by defining circular regions of interest (ROIs) within the central area of each sample. To increase the surface dose in breast cancer patients, commercial bolus material with a thickness of 0.5 or 1 cm is usually placed longitudinally on the patient's skin, from head to foot [20]. In clinical routine practice, a commercial bolus with a thickness of 1 cm is commonly utilized. The materials were positioned in the orientation typically used in clinical settings, and photographs were captured. For each material, the region of interest (ROI) was defined to ensure it remained entirely within 1 cm thickness. The ROI placement involved a circular area of 38.62 mm^2, positioned at five distinct locations.

The average HU values were used to analyze the radiological characteristics of the samples, whereas the standard deviation (STD) values provided insights into the uniformity of the printed samples.

2.3 Dosimetric measurements

In radiotherapy practice, depth dose distribution at the central axis is important to characterize a radiation beam. A complete analysis of all photon beam depth dose and profile parameters is essential for delivering radiation doses with higher accuracy. This also applies to patient-specific materials such as bolus, immobilization devices, or 3D printing materials. Dosimetric measurements were performed on the Varian DHX linear accelerator (Varian, Palo Alto, CA) and 6-MV photon beam. We used water phantom (Sun Nuclear, Melbourne, FL) to perform dosimetric measurements, such as PDD and dose profile measurements (Fig. 4). The analysis of the data was computer-controlled in phantom-specific software (Sun Nuclear SNC Dosimetry TM).

2.3.1 Percentage depth dose (PDD) measurements

The percentage depth dose (PDD) curve is an essential parameter for a specific type or energy of radiation. It denotes the ratio of the radiation dose at a given depth to the dose at a reference depth, represented as a percentage. In clinical radiotherapy, this reference depth is usually the point where the dose is maximized, known as dmax [21]. At dmax, the PDD value is expected to be 100%. To ascertain the PDD, both printed materials and a bolus were subjected to a 6-MV photon beam, utilizing a field

Fig. 3 Axial CT images were acquired to measure the mean HU and standard deviation (STD) values within the ROI of **a** FDM samples (PLA on the left, ABS on the right), **b** IM samples (PLA on the left, ABS on the right), and **c** commercial bolus
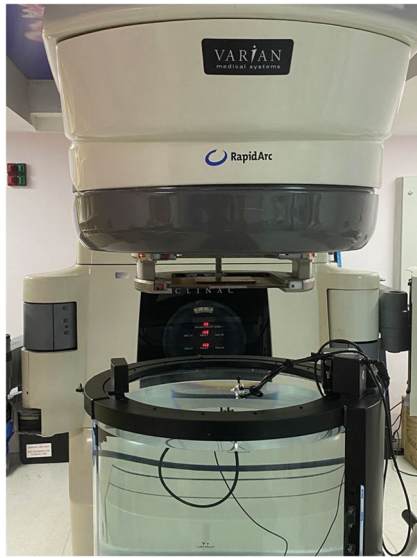
Fig. 4 Water phantom measurement setup

size of 10×10 cm^2. These measurements were performed along the central axis, with a 2-mm interval, beginning from the surface (0 mm) down to a depth of 300 mm. The depth dose readings taken in the commercial bolus were used as benchmark dose values for comparative purposes. PDD measurements for all materials were normalized to the maximum depth for each material to assess change at different depths.

2.3.2 Dose profile measurements

Megavoltage photon beams result in a significant dose increase within a few millimeters of tissues and organ. In radiotherapy patient treatment planning, it is essential to account for variations in the penumbra, particularly when delivering small off-center segments [22]. Penumbra is an important parameter that characterizes a beam. The term "penumbra" typically denotes the area at the periphery of a radiation beam where the dose rate undergoes rapid changes concerning the distance from the central axis [23]. Dose variations at different depths along the perpendicular axis to the beam were evaluated for each material. The effect of dose drop-off at the field edge (penumbra) was assessed. For 10×10 cm^2 field size at SSD = 100 cm, dose profile measurements were taken at maximum dose depth (dmax) and depth of 1.5 cm in the water phantom. Ion chamber measurements, moved in the in-plane direction within the water phantom along the gantry axis, were subjected to numerical analysis using the computer of the water phantom. Penumbra values are characterized as the distance between the 80 and 20% points of dose on a lateral beam profile.

2.3.3 RW-3 solid-water phantom measurements

Since percent depth dose (PDD) and dose profile measurements are relative, radiation transmittance evaluation measurements were also conducted using a measurement system comprised of a PTW Marcus ion chamber, a PTW Romeo electrometer, and a PTW RW3 solid water phantom. This system, utilized for absolute dosimetric measurements, is from PTW Freiburg, based in Freiburg, Germany. Both the electrometer and the ionization chamber have been calibrated and certified by the Çekmece Nuclear Research and Training Center Secondary Standard Dosimetry Laboratory.

Along the central axis, the radiation transmittance of each material was assessed. The irradiation experiments were carried out at various phantom depths, specifically at 1.5 cm (representing the maximum depth), as well as at 5.0, 10, and 20 cm. These were conducted for a field size of 10×10 cm^2, maintaining a source-to-surface distance (SSD) of 100 cm.

The experimental setup was consistently applied across all samples and the commercial bolus, as depicted in Fig. 5. The measurement values acquired from each material were then normalized against the values obtained from the commercial bolus to ensure comparability. The setup conditions outlined in Fig. 5 were applied for all materials, and each material underwent irradiation three times. Subsequently, the readings from the electrometer were averaged to ensure consistency and accuracy in the measurements.

3 Experimental results

3.1 Hounsfield unit (HU) analysis

The outcomes of the mean Hounsfield unit (HU) and standard deviation (STD) values acquired for the two methods at 0 (the center of the sample), 5 cm from the right and left sides of the center ($+5$ and -5), and 10 cm from the right and left sides of the center ($+10$ and -10) for each material are presented in Table 1.

3.2 Dosimetric measurements

The dose profile and PDD were compared with measurements using a water phantom. The results of PDD values are given in Table 2. The maximum relative dose, set at 100%, was normalized based on the maximum depth of penetration for each material.

PDD values are normalized to dmax along the beam central axis in the water phantom. PDD values are given in Fig. 6 for all samples.

Fig. 5 Radiation transmittance measurement setup. **a** The samples (PLA and ABS), **b** commercial bolus
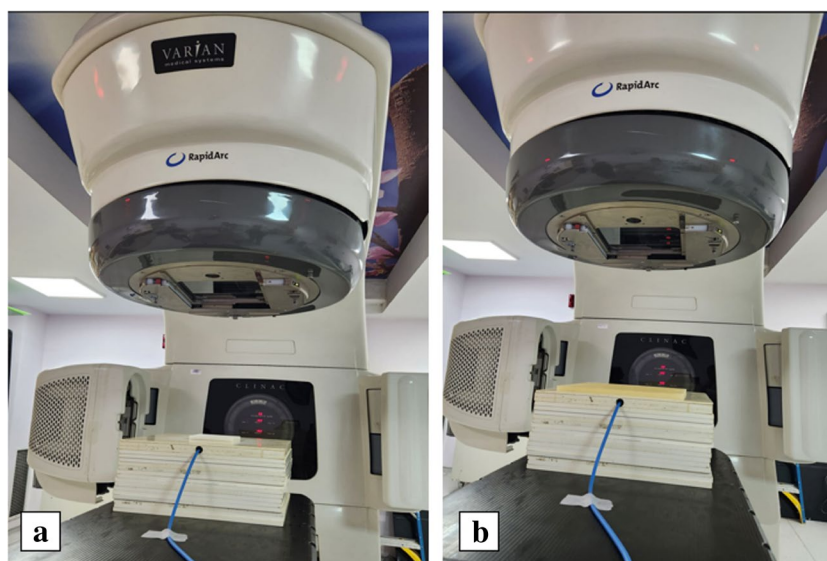

Table 1 HU (STD) values for samples

Sample	+10	+5	0	−5	−10
PLA (FDM)	27.56 (6.75)	14.48 (5.79)	20.53 (11.73)	−33.04 (6.16)	−38.48 (5.54)
PLA (IM)	149.81 (9.37)	149.91 (4.26)	146.02 (7.86)	137.52 (7.32)	127.79 (4.39)
ABS (FDM)	−17.33 (8.93)	−13.77 (5.18)	10.89 (12.51)	27.52 (7.26)	25.72 (8.53)
ABS (IM)	−67.35 (6.43)	−58.46 (5.09)	−55.32 (6.44)	−46.02 (6.56)	−47.34 (7.24)
BOLUS	28.85 (18.28)	17.11 (9.70)	26.14 (16.48)	−38.57 (9.08)	−31.08 (8.40)

Table 2 PDD values for samples

Sample	Dmax (cm)	Max (%)	D10 (%)	D20 (%)
PLA (FDM)	1.48	100	66.92	38.67
PLA (IM)	1.52	100	66.87	38.60
ABS (FDM)	1.48	100	66.91	38.49
ABS (IM)	1.51	100	66.77	38.52
BOLUS	1.52	100	67.06	38.75

An overview of the dose profile evaluation is shown in Table 3 and Figs. 7 and 8. The mean value between the left-side (penumbra (-)) and right-side (penumbra (+)) was calculated for each profile in Table 3.

Additionally, the comparison of profile measurements with commercial bolus for each material is provided in Table 4. SNC Dosimetry compare feature was used for profile evaluation. The compare feature provides numerical and graphical analyses of the difference between two different measurements of a processed scan on a point-by-point basis. The commercial bolus material was defined as a baseline for comparison. Analyses results and statistics for the selected comparison type (difference (baseline-comparison)-absolute difference: dose at scan 1 point-dose at scan 2 point) are shown in Table 4.

Dose measurements at different depths for 6-MV photon beams using Markus parallel plate ionization chamber. The average of three charge electrometer reading values (nC) are given in Table 5.

4 Discussion

In recent years, polymer materials have been the subject of extensive scientific research in the area of radiation oncology departments. Some of this research involves the design of patient-specific or quality-assured phantoms. Materials used as boluses in clinical practice must be non-toxic, easy to manufacture, durable, cost-effective, and flexible. Furthermore, the bolus should ensure a homogeneous dose distribution within the target volume. The suitability of tissue-equivalent 3D printing materials such as ABS, PLA, TPU, and polyvinyl acetate for use in radiotherapy has been confirmed [12, 24]. While 3D printers have started to be used in radiotherapy for various purposes, information regarding the interaction of printing materials with therapeutic radiation is limited. In the literature, the use of ABS and PLA materials as phantoms and bolus materials in a clinical setting is considered appropriate. However, determining how the filament used behaves against radiation is crucial. Measurements for
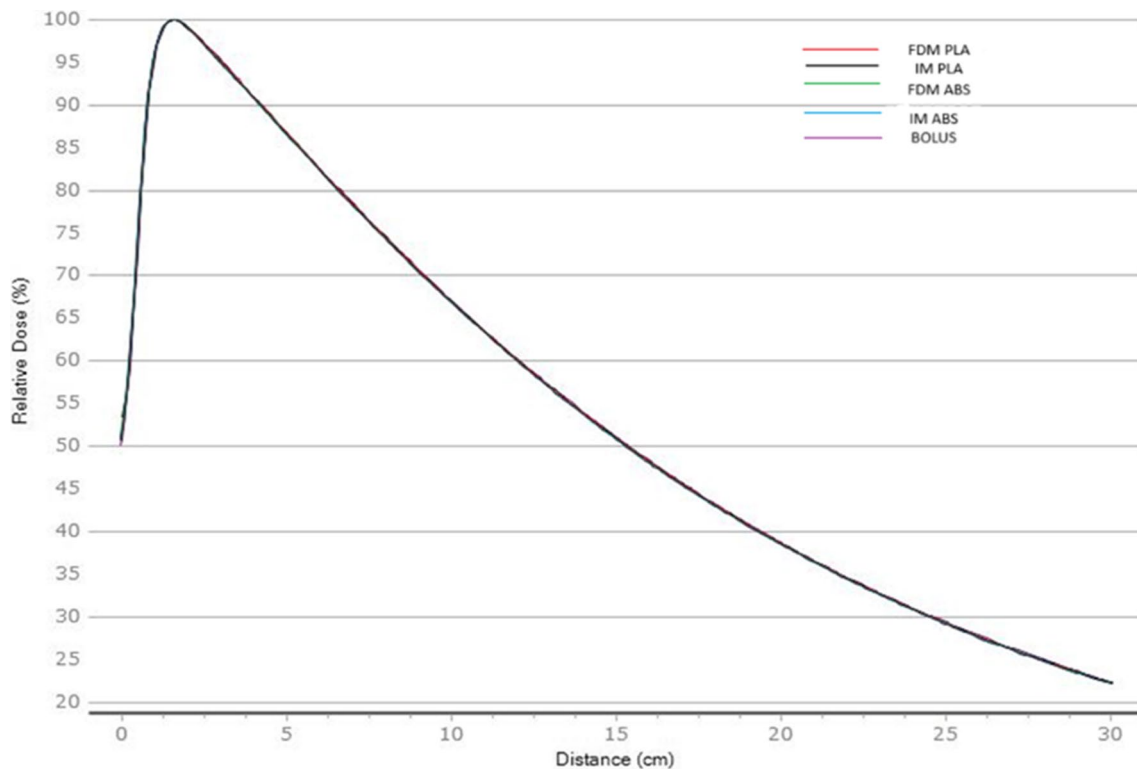
Fig. 6 The PDD variation as a function of depth dmax in a water phantom for all samples

Table 3 Evaluation of dose profile parameters

Sample	Penumbra (−) (cm)	Penumbra (+) (cm)	Symmetry (%)	Flatness (%)
PLA (FDM)	0.570	0.570	100.74	0.95
PLA (IM)	0.567	0.571	100.98	0.87
ABS (FDM)	0.566	0.569	101.11	0.89
ABS (IM)	0.565	0.568	101.54	0.80
BOLUS	0.589	0.596	100.47	0.92

this purpose may vary depending on the type of radiation used. The investigation of the use of filaments and 3D printing technology in radiotherapy is still in its early stages.

In this study, the impact of various manufacturing processes was assessed and contrasted regarding the dosimetric characteristics of PLA and ABS materials. The dosimetric properties that are the object of this research are HU, depth doses, dose profiles, and radiation transmittance.
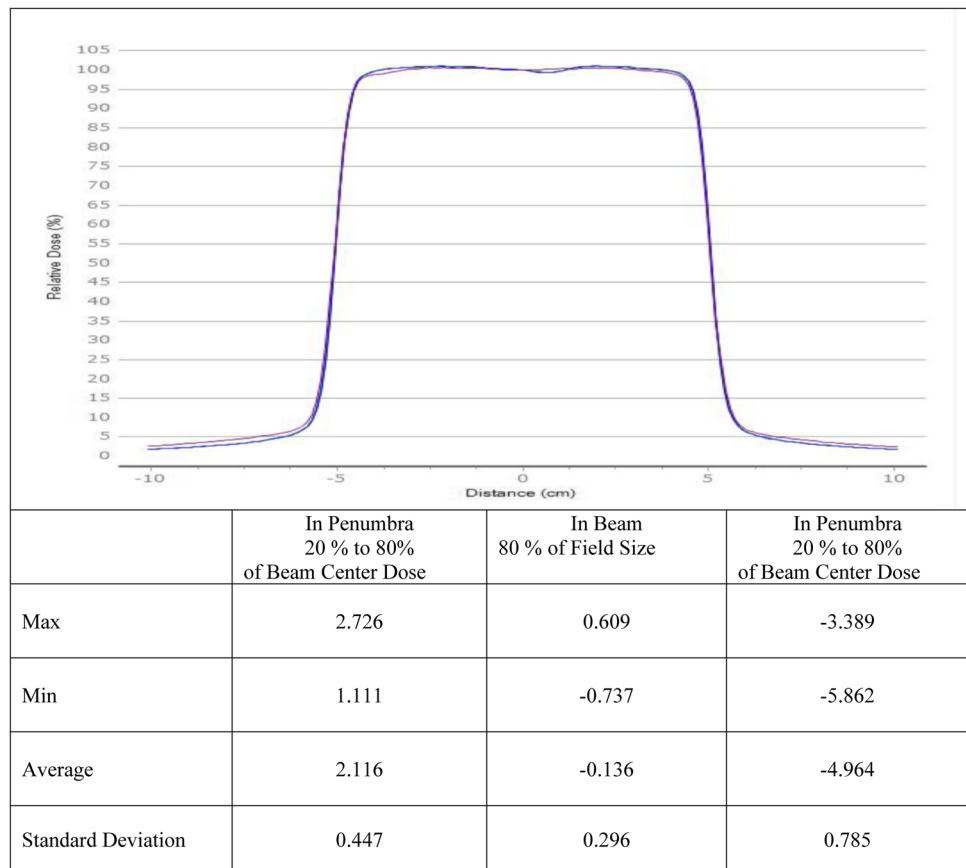
According to the literature, it is essential to assess materials before their clinical use. In our study, various routine dosimetric evaluations were conducted on the flat test materials before the development of 3D molding equipment using PLA and ABS materials for patients. HU values are typically between −1000 and +1000 in CT images. Özsoykal et al. obtained that HU values for cylindrical PLA samples were

between +73 HU and −450 HU. They concluded that materials produced with varying printing parameters using PLA filament may exhibit radiological properties resembling various soft tissues [25]. For fat and soft tissue it is between −70 and +40. It was found that the HU values of the materials obtained by both methods were not exactly the same and showed variations as seen in Table 1. The PLA material exhibited an average Hounsfield unit (HU) value, as indicated in Table 1, which closely resembled the HU value of water. For this research, we found samples between: +20.53 HU and −67.35 HU for mean soft tissues except the PLA IM sample. The closest HU values for the commercial bolus ranging from 28.85 to 31.08 were found to vary within the range of 27.56 to 33.04 for PLA (FDM).

In Köylü's study, electron densities and average HU values of RW3 and black ABS phantoms were determined to assess the homogeneity and smoothness of black ABS flat phantoms. The physical density of black ABS is 1.04 g/cm3, and its electron density relative to water is 0.953 g/cm3, while RW3's electron density relative to water is determined to be 1.005 g/cm3. The HU value for RW3 is 5, whereas for black ABS, it is −108 HU. HU readings at different points in both phantoms are very close and homogeneous [26].

In the study conducted by Jeong S. et al., 5 cm length cubes with varying densities of 50%, 75%, and 100% were 3D-printed using a 3D printer. The 3D printer employed an

Fig. 7 Dose profiles for maximum depth (1.5 cm) for all samples. The FDM PLA (red line), and the IM PLA (blue line) are shown in the figure
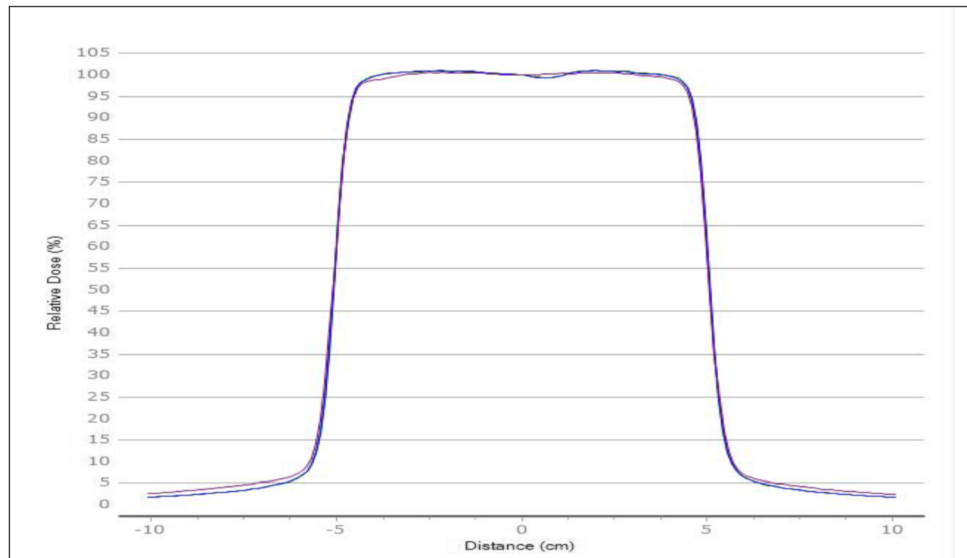

	In Penumbra 20 % to 80% of Beam Center Dose	In Beam 80 % of Field Size	In Penumbra 20 % to 80% of Beam Center Dose
Max	2.726	0.609	-3.389
Min	1.111	-0.737	-5.862
Average	2.116	-0.136	-4.964
Standard Deviation	0.447	0.296	0.785

additive method with an extruder to melt PLA during the experiment. Planning CT scans of the cubes were carried out using a CT simulator. The Hounsfield unit (HU) values for the 50%, 75%, and 100% density cases were recorded as -910, -860, and -10, respectively, although small errors were noted in the HU value results. This data serves as a reference for creating immobilization tools that can act as compensators and for developing realistic human phantoms that accurately depict the internal structures of the human body. The study holds significance for users of PLA-based 3D printers involved in planning projects related to radiation therapy [27].

The AAPM TG-40 report, which plays an important role in the assessment of changes in percentage depth dose data used in the evaluation of central axis dosimetric data in radiotherapy equipment, indicates a 2% data exchange between acceptance and measurement. Similarly, the same report sets a tolerance of 2% for the evaluation of profile data. With the advent of new technologies in radiotherapy, such as IMRT, the AAPM TG-142 report was published. According to this report, for IMRT, after all other quality control procedures have been completed, the treatment of a patient will proceed if the change in PDD and profile data at a depth of 10 cm is 1%. The AAPM TG-198 report published in 2021 also recommended these tolerances. Following these guidelines, the acceptance criteria for open-field depth dose data in treatment devices are met if the dose change falls within $\pm 1\%$ of the tolerance value [27, 28]. We have found that the relative dose difference for FDM and IM materials is smaller than 1.0% for 10×10 field sizes up to a depth of 30 cm along the central axis of the beam (Table 2, Fig. 5). We have also shown that dose profiles are symmetrical for the central beam axis for maximum depth dose in the water phantom where the difference was minimal. And the difference of width spread in intervals from -1 to 1 mm for penumbra regions (Figs. 6 and 7). In Table 5, the differences between the commercial bolus and all materials are shown. The measurements obtained using both techniques demonstrated a high degree of similarity ($< 0.8\%$) to those of the commercial bolus. The most significant deviation in dose was observed in the ABS (injection molded) at a depth of 20 cm. In their research, Zhang C. and colleagues explored the dosimetric properties of two 3D-printed filament materials, PLA and TPU. They compared these properties with various conventional bolus materials and RMI457 solid water. Their findings revealed that the percentage depth doses (PDDs) of the 3D-printed materials in comparison to RMI457 solid water varied by less than 3%. In contrast, for dental wax and SuperFlab gel materials, the variation was within 5%. These outcomes imply that PLA and TPU,

Fig. 8 Dose profiles for maximum depth (1.5 cm) for all samples. The FDM ABS (green line), and the IM ABS (blue line) are shown in the figure

	In Penumbra 20 % to 80% of Beam Center Dose	In Beam 80 % of Field Size	In Penumbra 20 % to 80% of Beam Center Dose
Max	-2.396	0.472	5.065
Min	-4.740	-0.634	2.521
Average	-3.909	0.025	4.150
Standard Deviation	0.698	0.243	0.802

Table 4 Penumbra results were obtained by comparing all materials with bolus at a maximum depth of 1.5 cm

Sample	Statistical values	In penumbra 20 to 80% of beam center dose	In beam 80% of field size	In penumbra 20 to 80% of beam center dose
FDM PLA	Max	0.089	0.260	4.489
IM PLA		1.213	0.827	−0.001
FDM ABS		3.357	0.903	0.400
IMABS		3.402	0.932	0.489
FDM PLA	Min	−2.540	−1.125	2.359
IM PLA		−0.437	−1.078	−1.999
FDM ABS		1.575	−1.044	−1.545
IMABS		2.579	−1.098	−1.637
FDM PLA	Average	−1.532	−0.238	3.589
IM PLA		0.582	−0.374	−1.204
FDM ABS		2.748	−0.326	−0.643
IMABS		2.579	−0.291	−0.687
FDM PLA	Standard deviation	0.846	0.333	0.634
IM PLA		0.611	0.413	0.731
FDM ABS		0.529	0.424	0.671
IM ABS		0.561	0.438	0.681

Table 5 Evaluation of radiation transmittance of the samples

Sample	1.5 cm	5 cm	10 cm	20 cm
PLA (FDM)	1.812	1.554	1.193	0.679
PLA (IM)	1.812	1.550	1.189	0.677
ABS (FDM)	1.815	1.555	1.194	0.679
ABS (IM)	1.814	1.558	1.197	0.681
BOLUS	1.813	1.553	1.190	0.678

when 3D-printed, are viable options for radiotherapy bolus materials [29].

To summarize the results of our study, no important differences were found in the dosimetric characteristics of PLA and ABS printed plates for two different production techniques. The agreement between the experimental values was very satisfactory, indicating that our experimental results can be applied to select different materials for our patients. However, it is important to note that our study has limitations, as we did not conduct measurements to identify variations with different field sizes and depths, as well as the effects of materials on dosimetry. Furthermore, the cost-effectiveness of preparing 3D-printed plates and the relatively widespread availability of 3D printers offer the potential for such materials to be utilized as bolus materials for patients undergoing radiation therapy. In routine radiotherapy applications, each material that can affect dose distribution in patients' treatments, all materials must undergo some quantitative tests before use. It is important to evaluate all materials that are produced by FDM or IM production methods used before the patients' treatments are evaluated for dose distribution and tissue equivalence.

5 Conclusion

This study rigorously investigated and contrasted the dosimetric properties of materials produced through two different manufacturing techniques with those of conventional commercial bolus material. Utilizing a 6-MV X-ray beam for experimental procedures, the findings indicate a close resemblance in the dosimetric properties of the tested materials to the reference bolus material. This alignment suggests their potential applicability in clinical settings. A significant highlight of this research is the insights it provides into the application of plastic injection molded materials in the realm of radiotherapy. Dosimetric evaluations of materials processed via plastic injection molding, specifically PLA and ABS, suggest these materials as viable candidates for the fabrication of 3D-printed boluses in radiotherapy treatments. This possibility marks a noteworthy advancement in the field, offering a more personalized and potentially more effective approach to patient care. However, it is crucial to underline the importance of conducting thorough dosimetric evaluations of these materials prior to their clinical application. Personalization of boluses for individual patients must be approached with caution, considering the inherent characteristics of the printing process and the variability of materials used. This step is vital to ensure the safety and efficacy of the treatment, aligning the properties of the 3D-printed boluses closely with the established standards of radiotherapy practices. By adhering to this protocol, the innovative use of 3D-printed materials in radiotherapy can be optimally leveraged to enhance patient outcomes.

Declarations

Competing interests The authors declare no competing interests.

References

1. N. Banaee, H.A. Nedaie, H. Nosrati et al., Dose measurement of different bolus materials on surface dose. J. Radiat. Res. **1**(1), 10–13 (2013). https://doi.org/10.12966/jrr.08.02.2013
2. L. Apipunyasopon, C. Chaloeiparp, T. Wiriyatharakij et al., Characterization of natural rubber as a bolus material for electron beam radiotherapy. Rep. Pract. Oncol. Radiother. **25**, 725–729 (2020)
3. M. Boopathi, D. Khanna, P. Venkatraman et al., Fabrication and dosimetric characteristics of silicon elastomer-based bolus using external beam radiotherapy. Asian Pac. J. Cancer Prev. **24**(1), 141–147 (2023). https://doi.org/10.31557/APJCP.2023.24.1.141
4. V. Vyas, L. Palmer, R. Mudge et al., On bolus for mega voltage photon an delectron radiation therapy. Med. Dosim. **38**(3), 268–273 (2013)
5. T.J. Ravine, Examining properties influencing infectious microbe associations with surfaces of four different thermoplastic radiation therapy masks. J. Med. Imaging Radiat. Sci. **52**(4), 576–585 (2021). https://doi.org/10.1016/j.jmir.2021.09.015
6. M.E. Mavili, H.I. Canter, B. Saglam-Aydinatay et al., Use of three-dimensional medical modeling methods for precise planning of orthognathic surgery. J. Craniofac. Surg. **18**(4), 740–747 (2007)
7. M. Fisher, C. Applegate, M. Ryalat et al., Evaluation of 3-D printed immobilisation shells for head and neck IMRT. Open J. Radiol. **4**(4), 322–328 (2014)

8. S.W. Kim, C.S. Kay, S.H. Son, A customized bolus produced using a 3-dimensional printer for radiotherapy. PLoS ONE. **9**(10), 1–8 (2014)

9. R.B. Kristiawan, F. Imaduddin, D. Ariawan et al., A review on the fused deposition modeling (FDM) 3D printing: filament processing, materials, and printing parameters. Open Eng. **11**(1), 639–649 (2021)

10. M.K. Rooney, S. Braunstein et al., Three-dimensional printing in radiation oncology: a systematic review of the literature. J. Appl. Clin. Med. Phys. **21**(8), 15–26 (2020)

11. Y. Lu, J. Song, X. Yao et al., 3D printing polymer-based bolus used for radiotherapy. Int. J. Bioprint. **7**(4), 414 (2021)

12. Y. Zhao, K. Moran, M. Yewondwossen et al., Clinical applications of 3-dimensional printing in radiation therapy. Med. Dosim. **42**, 150–155 (2017)

13. R. Tino, M. Leary, A. Yeo et al., Additive manufacturing in radiation oncology: a review of clinical practice, emerging trends and research opportunities. Int. J. Extrem. Manuf. **2**, 012003 (2020)

14. H. Tanabi, Investigation of the temperature effect on the mechanical properties of 3D printed composites. int. Adv. Res. Eng. J. **5**(2), 188–193 (2021)

15. U.K. Komal, B.K. Kasaudhan, I. Singh, Comparative performance analysis of polylactic acid parts fabricated by 3D printing and injection molding. J. Mater. Eng. Perform **30**, 6522–6528 (2021). https://doi.org/10.1007/s11665-021-05889-9

16. M.D. Zandi, R. Jerez-Mesa, J. Lluma-Fuentes et al., Study of the manufacturing process effects of fused filament fabrication and injection molding on tensile properties of composite PLA-wood parts. Int. J. Adv. Manuf. Technol. **108**(5–6), 1725–1735 (2020)

17. M. Lay, N. Laila, N. Thajudin et al., Comparison of physical and mechanical properties of PLA, ABS and nylon 6 fabricated using fused deposition modeling and injection molding. Compos. Part B **176**(1), 107341 (2019)

18. S. Szalai, B. Herold, D. Kurhan et al., Optimization of 3D printed rapid prototype deep drawing tools for automotive and railway sheet material testing. Infrastructures **8**(3), 43 (2013)

19. K. Gulliksurd, C. Stokke, A.C. Martinsen, How to measure CT image quality: variations in CTnumbers, uniformity and low contrast resolution for a CT quality assurance phantom. PhysMed. **30**(4), 521–526 (2014)

20. S. Aras, İO. Tanzer, T. İkizceli, Dosimetric comparison of super-flab and specially prepared bolus materials used in radiotherapy practice. Eur. J. Breast Health. **16**(3), 167 (2020)

21. F.M. Khan, *Physics of radiation therapy*, 3rd edn. (Lippincott Williams & Wilkins, Philadelphia, 2003)

22. P. Cherry, *Practical radiotherapy: physics and equipment*, 2nd edn. (Wiley-Blackwell, Hoboken, 2009)

23. E.B. Podgorsak, *Radiation oncology physics: a hand book for teachers and students* (International Atomic Energy Agency, Vienna, 2005)

24. E.E. Klein, J. Hanley, J. Bayouth et al., Task Group 142, American Association of Physicists in Medicine, Task group 142 report: quality assurance of medical accelerators. Med Phys. **36**(9), 4197–212 (2009). https://doi.org/10.1118/1.3190392

25. I. Özsoykal, R.B. Hüsemoğlu, A. Yurt, Radiological evaluation of the effects of printing parameters on 3D printed cylindrical LW-PLA samples: preliminary results. J. Med. Innov. Technol. **3**(2), 28–34 (2021)

26. M. Köylü, *Yogunluk Ayarlı Tüm Cilt Elektron Işınlama Tekniğinin Geliştirilmesi* (Ege Üniversitesi, Sağlık Bilimleri Enstitüsü, PhD Thesis, İzmir, Türkiye, 2020)

27. S. Jeong, M. Yoon, W.K. Chung et al., Preliminary study of the dosimetric characteristics of 3D-printed materials with megavoltage photons. J. Korean Phys. Soc. **67**, 189–194 (2015). https://doi.org/10.3938/jkps.67.189

28. J. Hanley, S. Dresser, W. Simon et al., AAPM task group 198 report: an implementation guide for TG 142 quality assurance of medical accelerators. Med. Phys. **48**(10), 830–885 (2021)

29. C. Zhang, W. Lewin, A. Cullen et al., Evaluation of 3D-printed bolus for radiotherapy using megavoltage X-ray beams. Radiol. Phys. Technol. **16**, 414–421 (2023). https://doi.org/10.1007/s12194-023-00727-0

Authors and Affiliations

Songül Çavdar Karaçam[1] · **Duygu Tunçman**[1] · **Tülin Şahin**[2] · **Şenol Şahin**[2] · **Şefika Arzu Ergen**[3] ·
Meltem Dağdelen[3] · **Ömer Erol Uzel**[3] · **Didem Çolpan Öksüz**[3] · **Ghada Almisned**[4] · **H. O. Tekin**[5,6]

✉ H. O. Tekin
htekin@sharjah.ac.ae; tekin765@gmail.com

Songül Çavdar Karaçam
songul.karacam@iuc.edu.tr

Duygu Tunçman
duygu.tuncman@iuc.edu.tr

Tülin Şahin
tulsah@kocaeli.edu.tr

Şenol Şahin
sensah@kocaeli.edu.tr

Şefika Arzu Ergen
ergenarzu@yahoo.com

Meltem Dağdelen
meltemdagdelen@windowslive.com

Ömer Erol Uzel
ouzel@iuc.edu.tr

Didem Çolpan Öksüz
didem.colpanoksuz@iuc.edu.tr

Ghada Almisned
gaalmisned@pnu.edu.sa

1   Radiotherapy Program, Vocational School of Health
    Services, Istanbul University-Cerrahpasa, Istanbul, Turkey

2   Mechanical Engineering Department, Kocaeli University,
    Izmit, Turkey

3   Radiation Oncology Department, Cerrahpasa Medicine
    Faculty, Istanbul University-Cerrahpasa, Istanbul, Turkey

4   Department of Physics, College of Science, Princess
    Nourah Bint Abdulrahman University, P.O. Box 84428,
    11671 Riyadh, Saudi Arabia

5   Department of Medical Diagnostic Imaging, College
    of Health Sciences, University of Sharjah, 27272 Sharjah,
    United Arab Emirates

6   Computer Engineering Department, Faculty of Engineering
    and Natural Sciences, Istinye University, Istanbul 34396,
    Turkey